

Electron-impact ionization of H₂ using a time-dependent close-coupling method

M. S. Pindzola, F. Robicheaux, and S. D. Loch

Department of Physics, Auburn University, Auburn, Alabama 36849, USA

J. P. Colgan

Theoretical Division, Los Alamos National Laboratory, Los Alamos, New Mexico 87545, USA

(Received 23 March 2006; published 15 May 2006)

Electron-impact ionization cross sections for H₂ are calculated using a nonperturbative time-dependent close-coupling method. In a standard frozen-core approximation, the six-dimensional wave function for the valence target electron and the incident projectile electron is expanded in products of rotational functions. The time-dependent Schrödinger equation for the two-electron system is then reduced to a set of close-coupled partial differential equations for the four-dimensional expansion functions in $(r_1, \theta_1, r_2, \theta_2)$ center-of-mass spherical polar coordinates. The nonperturbative close-coupling results are found to be over a factor of 2 lower than perturbative distorted-wave results, but in excellent agreement with experimental measurements, at incident electron energies near the peak of the total integrated cross section.

DOI: [10.1103/PhysRevA.73.052706](https://doi.org/10.1103/PhysRevA.73.052706)

PACS number(s): 34.50.Gb

I. INTRODUCTION

In the last couple of years, *ab initio* nonperturbative quantum methods have been developed to treat two continuum electrons moving in the field of a nonspherical diatomic molecular core, that is, a variant of Coulomb four-body breakup. Both the time-dependent close-coupling [1] and the exterior complex scaling [2] methods have produced total cross sections for the double photoionization of H₂ that are in reasonable agreement with experimental measurements [3,4], while the converged close-coupling [5,6] and the exterior complex scaling [7] methods have also been employed to calculate angular differential cross sections for the same electron correlation process. Furthermore, the time-dependent close-coupling method [8] has produced total cross sections for the electron-impact ionization of H₂⁺ that are in excellent agreement with experimental measurements [9], while the *R*-matrix with pseudostates method [10] has produced total cross sections for the electron-impact ionization of H₂ that are in excellent agreement with experimental measurements [11,12] in the near-threshold energy region.

In this paper, we apply the time-dependent close-coupling method to the Coulomb four-body break-up found in the electron-impact ionization of H₂. A standard frozen-core approximation is employed so that a six-dimensional wave function for the valence target electron and the incident projectile electron may be defined. The time-dependent Schrödinger equation for the quasi-two-electron system is then reduced to a set of close-coupled partial differential equations for the four-dimensional radial angular expansion coefficients in $(r_1, \theta_1, r_2, \theta_2)$ center-of-mass spherical polar coordinates. The close-coupled equations are solved for various values of total axial angular momentum M , total spin angular momentum S , total incident electron angular momentum, and total incident electron energy. Projections of time-evolved wave functions onto stationary-state bound orbitals yield ionization probabilities and cross sections. Comparisons of time-dependent close-coupling theory with experiment [12] are made for incident electron energies near

the peak of the cross section. Thus, we extend previous comparisons of nonperturbative theory [10] with experiment to higher incident electron energies. In addition, we carry out *ab initio* perturbative distorted-wave calculations using a recently developed configuration-average method [13] to assess the overall strength of electron correlation processes in electron ionization of H₂. In Sec. II we develop the time-dependent close-coupling theory for quasi-two-electron systems, in Sec. III we present electron-impact ionization cross section results for H₂, and in Sec. IV we conclude with a brief summary. Unless otherwise stated, all quantities are given in atomic units.

II. TIME-DEPENDENT CLOSE-COUPPING THEORY

The six-dimensional wave function Ψ^M for electron scattering from a valence target electron in a diatomic molecule is obtained by solving the time-dependent Schrödinger equation

$$i \frac{\partial \Psi^M(\vec{r}_1, \vec{r}_2, t)}{\partial t} = H_{\text{system}} \Psi^M(\vec{r}_1, \vec{r}_2, t), \quad (1)$$

where the nonrelativistic Hamiltonian is given by

$$H_{\text{system}} = \sum_i^2 \left(-\frac{1}{2} \nabla_i^2 + V(\vec{r}_i) \right) + \frac{1}{|\vec{r}_1 - \vec{r}_2|}, \quad (2)$$

and $V(\vec{r})$ is a single-particle interaction with the target nuclei and remaining core electrons.

The wave function Ψ^M for a given M symmetry is represented by an expansion in simple products of four-dimensional radial angular functions $P^M(r_1, \theta_1, r_2, \theta_2, t)$ and rotational functions

$$\Psi^M(\vec{r}_1, \vec{r}_2, t) = \sum_{m_1, m_2} \frac{P_{m_1 m_2}^M(r_1, \theta_1, r_2, \theta_2, t)}{r_1 r_2 \sqrt{\sin \theta_1} \sqrt{\sin \theta_2}} \Phi_{m_1}(\phi_1) \Phi_{m_2}(\phi_2), \quad (3)$$

where $\Phi(\phi) = \frac{e^{im\phi}}{\sqrt{2\pi}}$ and $M = m_1 + m_2$ in center-of-mass spherical polar coordinates. The angular reduction of the time-dependent Schrödinger equation, Eqs. (1) and (2), yields a set of time-dependent close-coupled partial differential equations given by

$$\begin{aligned} & i \frac{\partial P_{m_1 m_2}^M(r_1, \theta_1, r_2, \theta_2, t)}{\partial t} \\ & = T_{m_1 m_2}(r_1, \theta_1, r_2, \theta_2) P_{m_1 m_2}^M(r_1, \theta_1, r_2, \theta_2, t) \\ & + \sum_{m'_1, m'_2} V_{m_1 m_2, m'_1 m'_2}^M(r_1, \theta_1, r_2, \theta_2) P_{m'_1 m'_2}^M(r_1, \theta_1, r_2, \theta_2, t). \end{aligned} \quad (4)$$

The single-particle operator in the close-coupled equations is given by

$$\begin{aligned} T_{m_1 m_2}(r_1, \theta_1, r_2, \theta_2) = & \sum_{i=1}^2 [K(r_i) + \bar{K}(r_i, \theta_i) + A_{m_i}(r_i, \theta_i) \\ & + N(r_i, \theta_i) + V_{HS}(r_i, \theta_i)], \end{aligned} \quad (5)$$

where $K(r)$ and $\bar{K}(r, \theta)$ are kinetic energy operators [see Eqs. (7) and (8) of Ref. [8] for more details]. The axial angular momentum operator is given by

$$A_m(r, \theta) = \frac{m^2}{2r^2 \sin^2 \theta}. \quad (6)$$

The nuclear interaction operator is given by

$$N(r, \theta) = - \frac{Z}{\sqrt{r^2 + \frac{1}{4}R^2 - rR \cos \theta}} - \frac{Z}{\sqrt{r^2 + \frac{1}{4}R^2 + rR \cos \theta}}, \quad (7)$$

where $Z=1$ for H_2 and R is the internuclear separation. The Hartree-Slater potential operator is given by

$$V_{HS}(r, \theta) = V_{direct}(r, \theta) + \alpha V_{exchange}(r, \theta), \quad (8)$$

where the direct potential is given by

$$V_{direct}(r, \theta) = \sum_{\kappa} V_{\kappa}(r) P_{\kappa}(\cos \theta), \quad (9)$$

and the local exchange potential is given by

$$V_{exchange}(r, \theta) = - \frac{1}{2} \left(\frac{24\rho(r, \theta)}{\pi} \right)^{1/3}. \quad (10)$$

For H_2 ,

$$V_{\kappa}(r) = \int_0^{\infty} dr' \int_0^{\pi} d\theta' [\bar{P}_{1s0}(r', \theta')]^2 \frac{r'^{\kappa}}{r^{\kappa+1}} P_{\kappa}(\cos \theta') \quad (11)$$

and

$$\rho(r, \theta) = \frac{[\bar{P}_{1s0}(r, \theta)]^2}{2\pi r^2 \sin \theta}. \quad (12)$$

In Eqs. (8)–(12), α is an adjustable parameter used to achieve the experimental ionization potential for the valence electron orbital, $P_{\kappa}(\cos \theta)$ is a Legendre function, and $\bar{P}_{1s0}(r, \theta)$ is the ground-state wave function for H_2^+ with normalization given by

$$\int_0^{\infty} dr \int_0^{\pi} d\theta [\bar{P}_{1s0}(r, \theta)]^2 = 1. \quad (13)$$

Finally, the two-particle coupling operator is given by

$$\begin{aligned} & V_{m_1 m_2, m'_1 m'_2}^M(r_1, \theta_1, r_2, \theta_2) \\ & = \sum_{\lambda} \frac{r_{<}^{\lambda}}{r_{>}^{\lambda+1}} \sum_q \frac{(\lambda - |q|)!}{(\lambda + |q|)!} P_{\lambda}^{|q|}(\cos \theta_1) P_{\lambda}^{|q|}(\cos \theta_2) \\ & \times \langle (m_1, m_2) M | e^{iq(\phi_2 - \phi_1)} | (m'_1, m'_2) M \rangle, \end{aligned} \quad (14)$$

where $P_{\lambda}^{|q|}(\cos \theta)$ is an associated Legendre function.

The time-dependent close-coupling equations, Eq. (4), are solved using standard numerical methods to obtain a discrete representation of the radial angular functions $P_{m_1 m_2}^M$, and the one- and two-particle operators $T_{m_1 m_2}$ and $V_{m_1 m_2, m'_1 m'_2}^M$ on a four-dimensional lattice. Our implementation on massively parallel computers is to partition the radial coordinates (r_1, r_2) over the many processors, so-called domain decomposition. At time $t=0$ the radial angular expansion functions for the initial wave function of the scattering system are given by

$$\begin{aligned} & P_{m_1 m_2}^M(r_1, \theta_1, r_2, \theta_2, t=0) \\ & = \sqrt{\frac{1}{2}} [P_{1s0}(r_1, \theta_1) G_{k_0 l_0 M}(r_2, \theta_2) \delta_{m_1, 0} \delta_{m_2, M} \\ & + (-1)^S G_{k_0 l_0 M}(r_1, \theta_1) P_{1s0}(r_2, \theta_2) \delta_{m_1, M} \delta_{m_2, 0}], \end{aligned} \quad (15)$$

where the radial angular orbitals $P_{nlm}(r, \theta)$ are obtained by diagonalization of the one-electron Hamiltonian:

$$H_m(r, \theta) = K(r) + \bar{K}(r, \theta) + A_m(r, \theta) + N(r, \theta) + V_{HS}(r, \theta). \quad (16)$$

We note that the Gaussian wave packet $G_{k_0 l_0 M}$ is a function of the incident energy $\frac{k_0^2}{2}$ and the incident angular momentum l_0 . An implicit algorithm [see Eq. (11) of Ref. [8] for more details] is used to time-evolve the close-coupled equations for each value of M, S, l_0 , incident energy, and internuclear separation.

Probabilities for all the inelastic collision processes possible are obtained by $t \rightarrow \infty$ projection onto bound wave functions. Excitation probabilities are given by

$$\begin{aligned} \mathcal{P}_{nlm}^{MSI_0} = & 2 \sum_{m'} \left| \int_0^\infty dr_1 \int_0^\pi d\theta_1 \left| \int_0^\infty dr_2 \int_0^\pi d\theta_2 P_{m'm}^M(r_1, \theta_1, r_2, \theta_2, t) P_{nlm}(r_2, \theta_2) \right|^2 \right. \\ & \left. - \sum_{n'l'm'} \left| \int_0^\infty dr_1 \int_0^\pi d\theta_1 \int_0^\infty dr_2 \int_0^\pi d\theta_2 P_{m'm}^M(r_1, \theta_1, r_2, \theta_2, t) P_{n'l'm'}(r_1, \theta_1) P_{nlm}(r_2, \theta_2) \right|^2 \right|^2, \end{aligned} \quad (17)$$

and the ionization probability is given by

$$\mathcal{P}_{ion}^{MSI_0} = 1 - \sum_{nlm} \mathcal{P}_{nlm}^{MSI_0} - \sum_{nlm} \sum_{n'l'm'} \left| \int_0^\infty dr_1 \int_0^\pi d\theta_1 \int_0^\infty dr_2 \int_0^\pi d\theta_2 P_{mm}^M(r_1, \theta_1, r_2, \theta_2, t) P_{nlm}(r_1, \theta_1) P_{n'l'm'}(r_2, \theta_2) \right|^2. \quad (18)$$

The total ionization cross section is given by

$$\sigma_{ion} = \frac{\pi w_t}{4k_0^2} \sum_{M,S,l_0} (2S+1) \mathcal{P}_{ion}^{MSI_0}, \quad (19)$$

where w_t is the occupation number of the target subshell.

III. RESULTS

The time-dependent close-coupling (TDCC) method is used to calculate the electron-impact ionization cross section for H₂ at internuclear separations of $R=0.0$ and $R=1.4$, where the former is the separation for He and the latter is the equilibrium separation for H₂. We employ a $192 \times 16 \times 192 \times 16$ point lattice in $(r_1, \theta_1, r_2, \theta_2)$ center-of-mass spherical polar coordinates, with a uniform mesh spacing of $\Delta r=0.2$ from 0.0 to 38.4 in both r_1 and r_2 and a uniform mesh spacing of $\Delta\theta=0.0625\pi$ from 0.0 to π in both θ_1 and θ_2 . Diagonalization of the Hamiltonian of Eq. (16) for $m=0$ on a 192×16 point lattice using an α parameter of 0.58 in Eq. (8) yields a ground-state orbital with an ionization potential of 24.5 eV for $R=0.0$, while an α parameter of 0.34 yields a ground-state orbital with an ionization potential of 15.4 eV for $R=1.4$. The TDCC calculations for $R=0.0$ were made at an incident energy of 50 eV, while the TDCC calculations for $R=1.4$ were made at incident energies of 25, 50, and 75 eV. Partial cross sections $\sigma(M, S, l_0)$ were calculated for $M=(0, 1, 2)$, $S=(0, 1)$, and $l_0=(0, 1, 2, 3, 4, 5)$, where the coupled channels used for each M value are given in Table I. Partial cross sections $\sigma(l_0)$ were obtained from

TABLE I. Coupled channels used in the time-dependent close-coupling calculations.

$M=0$		$M=1$		$M=2$	
m_1	m_2	m_1	m_2	m_1	m_2
0	0	0	1	0	2
1	-1	1	0	2	0
-1	1	2	-1	1	1
2	-2	-1	2	3	-1
-2	2	3	-2	-1	3
		-2	3		

$$\sigma(l_0) = \sum_{M=-l_0}^{+l_0} \sum_{S=0,1} \sigma(M, S, l_0). \quad (20)$$

Partial cross sections for $-M$ are assumed equal to those for $+M$, while partial cross sections for $M \geq 3$ are assumed equal to those for $M=2$. To obtain total cross sections, the partial cross sections $\sigma(l_0)$ were extrapolated to high l_0 using a fitting function of the form

$$f(l_0) = a l_0^b e^{-c l_0}, \quad (21)$$

where a , b , and c are varied over an angular momentum range for $l_0 \geq 2$.

The configuration-average distorted-wave (CADW) method [13] is also used to calculate the electron-impact ionization cross section for H₂ at the same internuclear separations and incident electron energies at those used for the TDCC calculations. We employ a 1000×64 point lattice in (r, θ) center-of-mass spherical polar coordinates, with a uniform mesh spacing of $\Delta r=0.025$ from 0.0 to 25.0 in r and a uniform mesh spacing of $\Delta\theta=0.015625\pi$ from 0.0 to π in θ . By suitable choice of the parameter α , diagonalization of the Hamiltonian of Eq. (16) for $m=0$ on a 1000×64 point lattice yielded ionization potentials for the ground-state orbital as a function of R identical to those used before in the TDCC calculations. Partial cross sections were calculated for $l_0=(0 \rightarrow 9)$ and $m_0=(0 \rightarrow 4)$ and extrapolated to higher quantum numbers using the same procedures outlined above for the TDCC calculations.

The electron-impact ionization cross section results for H₂ at $R=0.0$ are presented in Table II. The CADW results are about 80% above experimental measurements [14], while the

TABLE II. Electron-impact ionization cross sections for He at an incident electron energy of 50 eV, for configuration-average distorted-wave (CADW) and time-dependent close-coupling methods (TDCC) ($1.0 \text{ Mb} = 1.0 \times 10^{-18} \text{ cm}^2$).

Method	Cross section (Mb)
CADW	42.7
TDCC	25.6
Experiment [14]	23.7 ± 1.1

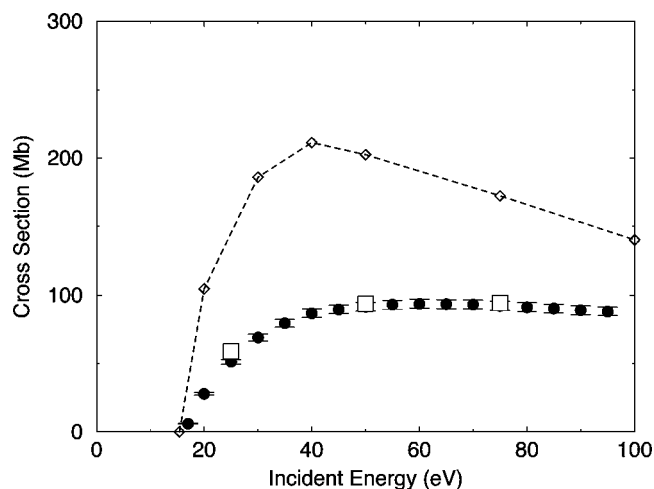


FIG. 1. Electron-impact ionization cross sections for H_2 . Opaque squares, time-dependent close-coupling results; connected open diamonds, distorted-wave results; solid circles, experimental measurements [12] ($1.0 \text{ Mb} = 1.0 \times 10^{-18} \text{ cm}^2$).

TDCC results are less than 1.0 Mb outside the experimental error bars. As has been shown in previous work [15] on the electron-impact ionization of He, atomic TDCC calculations are in excellent agreement with experimental measurements. On the other hand, atomic CADW calculations were found to be around 70% higher than experiment at 50 eV, falling to around 25% higher than experiment at 100 eV near the peak of the cross section.

The electron-impact ionization cross section results for H_2 at $R=1.4$ are presented in Fig. 1. The CADW results are over a factor of 2 higher than the experimental measurements [10] near the peak of the cross section, while the TDCC results

are in excellent agreement with experiment for each energy calculated. We note that the TDCC results at 25 eV are also in excellent agreement with previous nonperturbative R matrix with pseudostates calculations [10].

IV. SUMMARY

In conclusion, we have applied an *ab initio* nonperturbative method to the electron-impact ionization of H_2 . Using a standard frozen-core approximation, the total wave function for the valence target electron and the projectile electron is time evolved from an initial antisymmetrized product state of a stationary bound orbital and an incident wave packet to a final state that contains two continuum electrons moving in the field of a nonspherical diatomic molecular core. The time-dependent close-coupling calculations yield total cross sections that are over a factor of 2 lower than perturbative distorted-wave results, but in excellent agreement with experimental measurements for incident electron energies near the peak of the cross section. The substantial difference found between the perturbative and nonperturbative results indicates the presence of strong electron correlation processes in electron ionization of H_2 . In the future, we plan to continue the development of the time-dependent close-coupling method so that it can be applied to other more complex diatomic molecular systems.

ACKNOWLEDGMENTS

This work was supported in part by grants from the U.S. Department of Energy to Auburn University and Los Alamos National Laboratory. Computational work was carried out at the National Energy Research Scientific Computing Center in Oakland, California, and at the National Center for Computational Sciences in Oak Ridge, Tennessee.

-
- [1] J. Colgan, M. S. Pindzola, and F. Robicheaux, *J. Phys. B* **37**, L377 (2004).
 - [2] W. Vanroose, F. Martin, T. N. Rescigno, and C. W. McCurdy, *Phys. Rev. A* **70**, 050703(R) (2004).
 - [3] G. Dujardin, M. J. Besnard, L. Hellner, and Y. Malinovitch, *Phys. Rev. A* **35**, 5012 (1987).
 - [4] H. Kossmann, O. Schwarzkopf, B. Kammerling, and V. Schmidt, *Phys. Rev. Lett.* **63**, 2040 (1989).
 - [5] A. S. Kheifets, *Phys. Rev. A* **71**, 022704 (2005).
 - [6] A. S. Kheifets and I. Bray, *Phys. Rev. A* **72**, 022703 (2005).
 - [7] W. Vanroose, F. Martin, T. N. Rescigno, and C. W. McCurdy, *Science* **310**, 1787 (2005).
 - [8] M. S. Pindzola, F. Robicheaux, and J. Colgan, *J. Phys. B* **38**, L285 (2005).
 - [9] B. Peart and K. T. Dolder, *J. Phys. B* **6**, 2409 (1973).
 - [10] J. D. Gorfinkiel and J. Tennyson, *J. Phys. B* **38**, 1607 (2005).
 - [11] E. Krishnakumar and S. K. Srivastava, *J. Phys. B* **27**, L251 (1994).
 - [12] H. C. Straub, P. Renault, B. G. Lindsay, K. A. Smith, and R. F. Stebbings, *Phys. Rev. A* **54**, 2146 (1996).
 - [13] M. S. Pindzola, F. Robicheaux, J. A. Ludlow, J. P. Colgan, and D. C. Griffin, *Phys. Rev. A* **72**, 012716 (2005).
 - [14] R. G. Montague, M. F. A. Harrison, and A. C. H. Smith, *J. Phys. B* **17**, 3295 (1984).
 - [15] M. S. Pindzola and F. J. Robicheaux, *Phys. Rev. A* **61**, 052707 (2000).